Received: 16 September 2022 | Revised: 22 November 2022 | Accepted: 14 December 2022

DOI: 10.1002/pen.26239

RESEARCH ARTICLE

POLYMER ENGINEERING AND SCIENCE WILEY

Preparation and characterization of hydrophilic and water-swellable elastomeric nanocomposites

Bismark Mensah | **Emmanuel Oduro**

Department of Materials Science and Engineering, CBAS, University of Ghana, Legon, Ghana

Correspondence
Bismark Mensah, Department of Materials Science and Engineering, CBAS, University of Ghana, Legon, Ghana.
Email: bismarkmensah@ug.edu.gh

Abstract

Highly polar and hydrophilic polymers; ethylene-vinyl acetate (EVA), epichlorohydrin rubber (GECO), and polyethylene oxide (PEO) reinforced with fillers (carbon black (CB) and/or Silica) were used to prepare water-swellable rubber nanocomposites. The study showed that although the high content of the GECO delayed vulcanization of the corresponding compounds, the sample filled with desired ratio of GECO/PEO/EVA or GPE, cross-linked with peroxide exhibited the highest swelling performance of ~150%. The samples exhibited good re-usability performance in the re-swollen test, after drying. At prolonged water swelling, the tensile strength dropped drastically for compounds with high content of the GPE, due to weak filler-matrix interactions. On the other hand, the incorporated GPE also increased the rebound resilience (%) property which is a key requirement in green tire fabrication. For example; peroxide cured sample coded SR3 (GPE-15 phr CB) obtained ~30% resilience in non-swollen state and ~53.5% after 1440 min of water-swelling, which represents a dramatic development of over ~78% in rebound resilience. Thus, a proper balance between the GPE content, curing agent and the reinforcements may guarantee high water-swelling performance and mechanical properties integrity for multifunctional applications such as wound healing, structural works, water collection from oil spillages, and for the development of water-based sensors.

KEYWORDS

composites, elastomers, mechanical strength and resilient, rubber, swelling, volume expansion, water

1 | INTRODUCTION

The unique properties of visco-elastic polymers which include; strength-to-weight ratio, impact resistance, wear resistance, corrosion resistance, and others can be enhanced when they are reinforced with desired concentration of fillers.[1,2] The popular reinforcement mechanism is by either filler-filler or polymer-filler interactions.[1–3] In terms of mechanical properties, these fillers can actually absorb and transfer loads at the filler-matrix interface[1,2,4] whereas for electrical conductivity features, conductive fillers are controlled to create percolated pathways for electrons to flow within the matrix.[1,2,4] Therefore, there is an increase rate of interests of application of elastomer-fillers compositions, including; dielectrics, sensors and actuators,[5–10] flexible electronics, heat sinks and gaskets,[11–14] electromagnetic shields,[15] elastomeric quantum dots materials,[16] and many attractive areas. Over the years, water swellable elastomer (WSE) class of polymers have received

great attention in academics and industry for several purposes like sealing or expandable materials used in civil constructions for avoiding water leakages in pipes and working joints in concrete,[17–20] oil and gas drilling fields[19,21,22] and water-responsive and mechanically adaptive sensors[23–26] etc. As such, a wide range of elastomers have been examined for the water-swellability, some of which include; polychloroprene rubber (CR), polyoligomeric silsoxane (PDMS), acrylic rubbers (AR), natural rubber (NR), ethylene-propylene-diene monomer (EPDM), acrylonitrile butadiene rubber (NBR), and polybutadiene rubber.[1,2,17] Generally, elastomers do not swell in water irrespective of their polarities. Vaniev et al.[27] carried a study on the water swelling behaviors of NBR, it was observed that the polar moieties (acrylonitrile content) of NBR did not have any serious influence on it water-swelling properties. Thus, water swelling of elastomers can only be achieved through careful engineering.[19,21,22] In this regard, two methods have been established for engineering WSE, they include; chemical and physical method.[17,19,28] The physical method of preparing WSE include the use of solid/melt blending approach to prepare an elastomer by incorporating hydrophilic substances such as sodium salt of polyacrylic acid, polyethylene glycol, polyvinyl alcohol, carboxymethyl cellulose, and many others.[17,19,28,29] These classes of polymers are popularly called super absorbent polymers (SAP) which are cross-linked hydrogel. Earlier on Wang et al.[28] successfully used the physical method to prepare a WSE composite by filling CR elastomer with cross-linked sodium polyacrylate (CSP) and PEO. Since then, many works have been reported by using the physical method of fabrication of WSE.[29–31] The chemical methods include; interpenetrating polymer network (IPN) technology, grafting technology, and the use of compatibilizers.[17,19,28] In particular, the grafting polymerization is very famous approach used to graft polar chains on many hydrophobic polyolefin polymers.[17,19] However, the use of compatibilizers during grafting process has been found to increase leaching, filler dispersions and overall enhancement of water-swelling performance.[17] Notably, the chemical method was developed to overcome the poor interfacial interactions between the guest polymer SAP and the main matrix. Although, WSE have shown promising markets demands, however several associated problems have been reported. For example, highly cross-linked WSE are disadvantaged due to their poor biodegrading properties.[17,19] In addition, most WSE are prepared through complex routes and could be expensive, should they be patronized in the future markets.[17–19] Moreover, the use of WSE at high temperature and pressure environment is not well established.[17–19] Another serious challenge with WSE is their poor mechanical integrity. Saijun et al.[18] reported a decrease in mechanical properties of prepared WSE of NR-SAP, although with an increasing water swelling properties. Similar results of poor mechanical properties of WSE materials were reported quiet recently.[17,19] Going forward, there is the need to continue to investigate WSE to address issues relating to their engineering, so as to brighten their future potentials. This present work seeks to investigate different ways to preparation WSE with excellent water swelling performance and yet with suitable physico-mechanical integrity. The WSE was prepared by melt mixing technique after controlling the microstructure of several elastomers using hydrophilic systems (SAP) like diaper polymer gel (CSP) and blends of ethylene-vinyl acetate (EVA), epichlorohydrin rubber (GECO) and polyethylene oxide (PEO) in the presence of fillers and different curing agents. The effect of the SAP on the physico-mechanical properties: physical observation, water swelling behavior, tensile properties, resilience, hardness, crosslinking density of the optimized designs were carefully examined and clearly presented.

2 | EXPERIMENTAL DESIGN

2.1 | Chemicals and compound formulation

In this study, natural rubber, epoxidated natural rubber (ENR), polybutadiene rubber (BR), carboxylated nitrile rubber (XNBR) with CAN: 26.43%, ethylene-vinyl acetate (EVA), and epichlorohydrin rubber (Hydrin T3108) (GECO) were purchased from Doo Man Co. Ltd, South Korea. The GECO is a terpolymer of epichlorohydrin (CO), ethylene oxide (EO), and allyl glycidyl ether (AGE). This terpolymer contains 18–20% of chlorine (epichlorohydrin), 6%–8% of double bonds (AGE), and a high amount of ethylene oxide (EO). The diaper polymer (cross-linked sodium polyacrylate (CSP), and Polyethylene oxide (Mw ~ 600,000) were purchased from Sigma-Aldrich. Carbon black N550 (particle size: 40–48 nm, with the specific surface of 95–105 m^2/g), Silica (Z175MP) were obtained from IDONG TECH. The curatives; zinc oxide (ZnO), Stearic acid (SA), Sulfur (S), tetramethyl thiuram disulfide (TMTD), and N-cyclohexile 2-Benzotiazole Sulfonamide (CZ), peroxide curing system, and triallyl isocyanurate (TAIC) were all obtained from Info. Chem. Co. Ltd. Various compositions were formulated/design and all measured were expressed in part per hundred of rubber (phr). The different compounds designs are presented in Table 1.

TABLE 1 The compound formulation/design expressed in phr

			Type C				
Samples/code	**Type A**	**Type B**	**SR1**	**SR2**	**SR3**	**SRX**	**SRN**
XNBR/ENR	70	70	-	-	-	40	-
NR	-	-	-	-	-	-	-
BR	-	-	-	-	-	20	10
GECO	-	-	70	40	40	30	40
EVA	-	-	-	20	10	-	5
PEO	30	-	30	40	50	10	45
CSP	-	30	-	-	-	-	-
ZnO	3	3	5	3	3	5	5
TMTD	1	1	1	-	-	1	1
CBS (CZ)	0.5	0.5	0.5	-	-	0.5	0.5
N550	20	20	20	15	15	30	25
Silica	-	-	-	-	-	5	3
Silane	-	-	-	-	-	1	1
Sulfur	2.0	2.0	2.0	-	-	2.0	2.0
SA	1.4	1.4	1.4	1.5	1.5	1.4	1.4
DCP	-	-	-	2.2	2.2	-	-
TAIC	-	-	-	1	1	-	-

Note: Phr (part per hundred part of rubber), CZ (N-cyclohexyl-2-benzothiazoly-sulfenamide), TMTD (tetramethlythiuram disulphide), S (sulfur), SA (Stearic acid), ZnO (Zinc Oxide), triallyl isocyanurate (TAIC).

2.2 | Preparation of water-swellable elastomer

Three different polymer matrices/blends were engineered by tailoring their microstructure to be hydrophilic and water-absorbable. They include; type A: (pure non-polar (NR) and pure polar rubber (XNBR or ENR) filled with PEO) type B: (pure non-polar (NR) and pure polar rubber (XNBR or ENR) filled with CSP), type C: (A blend of pure polar (GECO and/or EVA) and non-polar rubber matrix (BR) with a PEO). Samples SR1–SR3 and SRX and SRN are samples prepared from type C. But samples SRX and SRN were prepared to overcome mechanical strength instabilities observed among samples SR1–SR3. All samples were prepared through the melt blending method by using internal mixer machine at 60 r/min rotor speed with a fill factor of 80%. The raw polymer materials were masticated and mixed with plasticizers, accelerating agent, reinforcing fillers, and later the SAP components (PEO or CSP) for 3 min at about 80°C. The samples were then mixed homogenously over a two-roll mill (QM300, QMESYS, YUNTECH Co. Ltd. South Korea) for 5 min after incorporating the sulfur or the peroxide curing additives. The samples were later cured using a rheometer machine at a temperature of 160°C and the curing information obtained was used to cure the samples in a hot press machine (model: TO-200, TESTONE. YUNTECH Co. Ltd. South Korea) that operates at pressure of 25 Tons. Different molds were used for curing the samples, for example, metal mold of 15 cm x 15 cm dimension with 2 mm thickness was used to cure samples from which the swelling and tensile tests samples were prepared.

3 | CHARACTERIZATION

3.1 | Vulcanization properties of compounds

The curing properties of the WSE composites cured with sulfur and peroxide curing agents in the presence of carbon black (CB) and/or silica and the hydrophilic components were studied by using an oscillating-die rheometer (MDR, model: PDR2030, TESTONE. Co. Ltd., South Korea) operating at 160°C. The various curing parameters including; maximum torque (M_H), minimum torque (M_L), change in torque ($\Delta M = M_H - M_L$), onset of cure time (t_{s2}), optimum cure time (t_{90}), and curing rate index ($CRI = 100/(t_{90} - t_{s2})$) of the various compounds were carefully extracted from the rheo-curves, analyzed and presented.

3.2 | Hydrophilic behavior of WSE compounds

Hydrophilic or water wetting test is usually done with contact angle measured, however in this present work, a water wetting test was achieved by carefully dropping a small amount of de-ionized water onto a clean and dry surface of a vulcanized WSE composites sheets by using 1 mm needle in a syringe. A camera positioned at one place was used to take the pictures of the water drop after 1 min. In principle, a spread of the water droplet depicts a high energy surface (hydrophilic) while a failure to spread after some period of time marks a sign of hydrophobic or low surface energy. The result obtained from this analysis was compared with a more hydrophobic surface like aluminum oil and mylar film at the same conditions.

3.3 | Water-swelling ratio and volume expansion test

In this test, the samples were cut into square shapes of about 2 cm × 2 cm with a thickness of ~2 mm thickness. The initial weight of sample and their corresponding dimensions were recorded. The samples were swollen in the water and their final weights were monitored at certain periods for almost 3 weeks. At each period, the change in dimensions was quickly monitored using micrometer screw guage. The equations (1–3) were used to calculate their respective degree of water swelling (%), water swelling rates and volume expansion, VE (%) of the various samples respectively.

$$\text{Swelling degree}(\%) = \left(\frac{W_i - W_f}{w_i}\right) * 100 \quad (1)$$

The water absorption rates of the various compounds at 1–7 days were computed by using the Equation (2)[32]; SR_7 and SR_{eq} represents the water-swelling ratio at 7 days and the equilibrium water-swelling respectively.

$$Sr = \frac{SR_7}{SR_{eq}} \quad (2)$$

The volume expansion was computed using Equation (3), where V_i and V_s are the respective initial and volume swollen sample.

$$VE(\%) = \frac{v_i - v_S}{V_i} * 100 \quad (3)$$

Re-usability test was done after the water-swollen samples were fully dried in the sun and were re-equilibrated in water following the same swelling method explained above. Their new degrees of swelling and volume expansion were calculated using Equations (1) and (3).

3.4 | Chemical analysis of compounds

Fourier transform infrared (FT-IR) spectra of the various compositions were recorded on a Jasco FT-IR-4200 spectrophotometer (USA) obtained from Chemistry Department, University of Ghana. The chemical structural properties observed have been presented.

3.5 | Effect of hydrophilicity and water-swelling on mechanical properties

3.5.1 | Crosslinking density

Swelling experiments of vulcanized WSE composites were performed by equilibrating them in toluene at room temperature for 48 h. The swelling degree Q_r was calculated using the relation

$$Q_r = \frac{W_s - W_i}{W_i} \quad (4)$$

where *Wi* is the weight of the rubber sample before immersion into the solvent, W_s weights of the sample in the swollen state. The elastically active network chain density (the crosslink density, *N*), was calculated from Flory-Rehner equation given by Equation (5).[33]

$$-\left[In(1-\nu_r) + \nu_r + \chi_1 \nu^2 r\right] = \nu_s \left[\nu_r{}^{1/3} - \nu_r/2\right] N \quad (5)$$

where $V_r(1/Q_r)$ the volume fraction of polymer in the swollen gel at equilibrium, V_s is the molar volume of the solvent (106.3 ml/mol for toluene) and χ_1 is the polymer-solvent parameter determined from Bristow-Watson Equation (6),[34] where

$$\chi_1 = \beta_1 + (\nu_s/RT)\left[\delta_s - \delta_p\right]^2 \quad (6)$$

where β is the lattice constant, usually taken as 0.34, V_s is the molar volume of solvent, R is the universal gas constant, T is the absolute temperature and δ is the solubility parameter and the subscripts s and p refer to the swelling agent and polymer, respectively. The values for the δ_s and δ_p were 8.91[35] and 8.10[36] respectively, while the χ_1 was calculated to be 0.368.

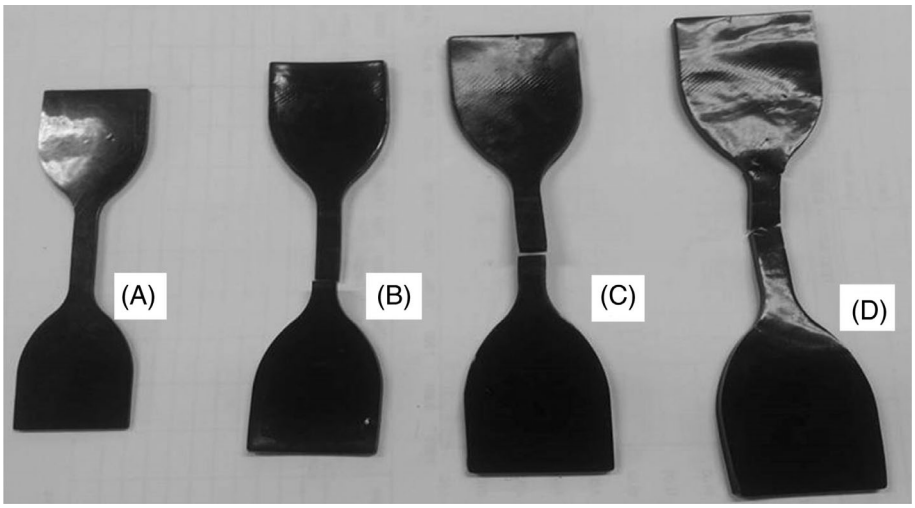

FIGURE 1 Typical dumbbell-shaped type C samples (SR3) in non-swollen and swollen state for tensile testing. (A) Non-swollen state(B) after 1 min of water swelling (C) 1 h after water swelling and (D) 24 h after water swelling.

3.5.2 | Tensile properties

The tensile strength (TS) measurement for the cured WSE composites for the swollen and non-swollen state was carried out according to ASTM D412 standard by using (QM100s machine, QMESYSTEM, South Korea) at a cross-head speed of 500 mm/min and at 25°C temperatures. At least three samples were tested for each of the compositions and averaged. The optimum swelling time for performing the tensile test for the case of desired samples (type C) which were swollen in water was: 1 min, 1 h, and 1 day. TS on extended swollen times was not successful as the highly swollen samples could not be held by the clamp of the tensile machine. The representative TS samples for swollen and non-swollen conditions are shown Figure 1.

3.5.3 | Rebound resilience study

The elastic behavior (rebound resilience) of the of type C samples swollen in water for 0 min, 1 h, and 24 h was analyzed by using DIN resilience tester (DIN 53512 and ISO 4662), QMESYS acquired from YUNTECH Co. Ltd, South Korea. The sample is cylindrical in shape with thickness of ∼12 mm and ∼ 16 mm diameter. The methods involved was reported by earlier Mensah et al.[37] Briefly, to eliminate internal defects in the sample, the hammer part of the instrument was initially used to hit the surface of sample five times. Per the (DIN 53512 and ISO 4662) standard, any hits after 5th hit, could be recorded as the rebound resilience value. Hence in this present work, the 7th hit was taken as measurement after the 5th hit.

3.5.4 | Hardness (shore a) property

A constant loader hardness tester (Shore A) (QMESYS, YUNTECH Co. Ltd) with load 5 kg. South Korea was used to test the hardness of the swollen (1 and 24 h) and non-swollen WSE composite vulcanizates. Three samples with cylindrically shaped, with thickness of ∼12 mm and ∼ 16 mm diameter were tested and averaged for each composition.

3.5.5 | Wear resistance test

The abrasiveness of the various desired WSE composites in or without the presence of water was investigated by using the DIN abrasion machine (QMESYS Co. Ltd, South Korea). A cylindrical-like rubber test specimen (∼6 mm thickness and 16 mm diameter) were made and abraded against an abrasive surface mounted on a rotating cylindrical drum. The amount of rubber reduced in the specimen relative to its original weights due to abrasion is measured. At least, for each composition, three samples were tested and averaged.

3.6 | Thermal degradation property

The effect of the hydrophilic components (GECO/PEO/EVA), simply GPE, filler reinforcement, and the nature of curatives on the thermal degradation resistance of the various water-swellable composites was examined by using thermal gravimetric analysis (TGA). The TGA instrument used is SDT Q600-TA Instruments obtained from the Department of Material Science and Engineering School, University of Ghana. The conditions used include a nitrogen medium, equilibrium temperature of

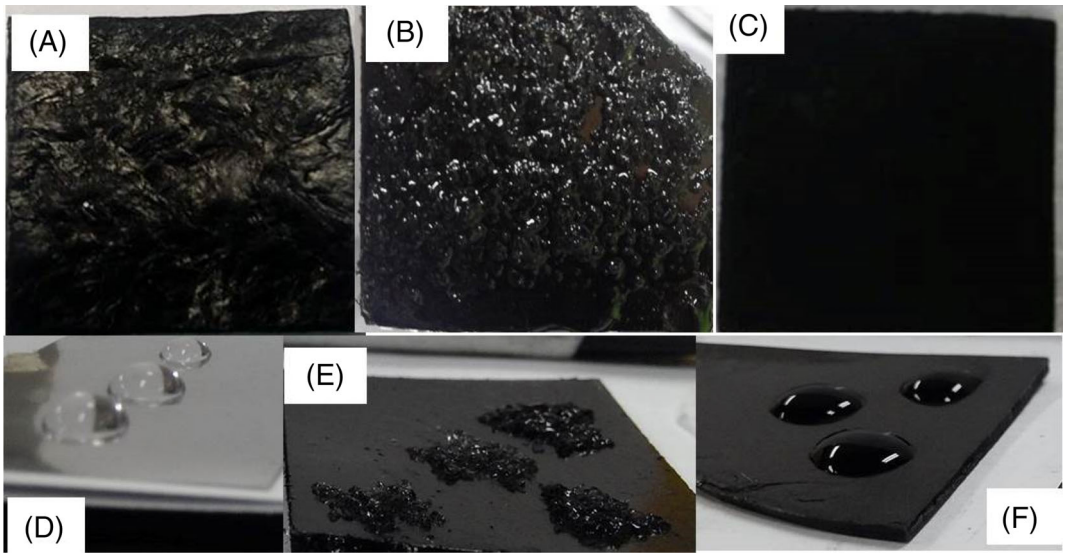

FIGURE 2 Surface morphology of type a, B, and C compositions; (A) type a (B) type B (C) type C. contact angle measurements of samples after water droplets onto; (D) aluminum foil (E) type B sample and (F) type C sample.

about 25°C and a heating rate of 10°C/min to a maximum temperature of 800°C. The weight residue (%) was used to explain the respective thermal resistance behaviors.

4 | RESULTS AND DISCUSSIONS

4.1 | Physical observation and water wettability study

The physical appearance of the representative samples of type A, B, and C are compared together in Figure 2A–C, respectively. The type A samples showed a swelling behavior (<2%), with a weak tearing strength shown in Figure 2A. With a slight tearing force, type A samples easily got broken. Although, type B composition showed great swelling behavior but was highly unstable because the guest hydrophilic polymer (CSP) migrated out of the bulk matrix to the observing surface of the composition, after swelling (Figure 2B).

This implied, there was poor interaction between the main matrix and guest polymer.[19] As seen in Figure 2C, the type C sample exhibited high viscoelastic properties with a smooth surface morphology and was able to absorb over 2% of water. This was an indication of effective compatibility between hydrophilic component (PEO), the filler, curatives, and the kind of matrices/blend used in presence of the other additives. The water wetting behavior of hydrophobic aluminum foil and the representative samples of type B and C are shown in Figure 2D–F respectively. In 1 min after dropping the water onto the surfaces of the matrices, spreading occurred and as clearly seen, the water wetting behavior

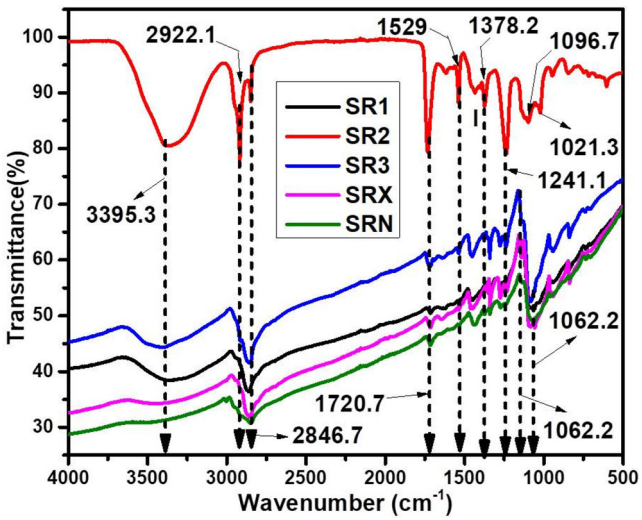

FIGURE 3 FTIR analysis of the various compositions (SRI, SR2, SR3, SRX, and SRN)

of the samples followed the decreasing order of; type B > type C > aluminum foil. Higher wetting behavior is associated with lower contact angles as observed by Dehbari et al.[22] upon incorporating poly(acrylic acid) into PDMS. Accordingly, the expected contact angle values may decrease in the same order as the wetting properties. Therefore, it was observed that all the compositions (A–C) generally exhibited hydrophilic behavior, with good wetting properties. However, due to complementarity purpose of water swelling and mechanical integrity, type C was preferred, and so extended compositions of type C (SR1, SR2, SR3, SRX, and SRN) were prepared and subjected into further studies.

4.2 | Chemical structure analysis of WSE composites by FTIR

Figure 3 is the FTIR analysis for the desired (type C) vulcanizates of the WSE compounds. The sample SR1, SR2, and SR3 showed O–H stretching vibrations around ~3347, ~3395, and ~3420 cm^{-1} respectively. The intensity of these peaks was stronger for SR2 while it broadened for rest of the compounds. This may be due to the presence of excess water moisture in the microstructure of SR2, probably absorbed from the air.[38] A characteristic sharper absorption band appearing at ~2922 cm^{-1} for SR2 may be due to contributions mainly from ethylene group, both from PEO or EVA.[39] As the content of EVA was reduced, this peak shifted to lower wavenumber (2855–2862 cm^{-1}) for the remaining sample.

The absorbance peak at 1724 cm^{-1} could be a stretching vibration of carbonyl group (O=C(CH_3)-O) coming from EVA.[39] This peak was sharper for SR2 containing the highest amount of EVA (20 phr), less sharp for SR3 (10 phr of EVA), and much weaker for SRN (5 phr of EVA). This characteristic peak seems to disappear or becomes weaker for SR1 and SRX which do not contain EVA. In addition, the peak appearing at ~1374 cm^{-1} may be coming from the wagging vibration of $–CH_3$ group in crystalline PEO unit.[40] This particular peak shifted to ~1341 cm^{-1} for SR3 and SRX, while it seems to disappear for sample SR1 which contained only a smaller content of the PEO (10 phr). The absorption bands around ~1241 cm^{-1} may be ether groups coming from EVA[39] and it is very sharper for SR2 for the same reason of the EVA content. The absorbance peak at ~1076–1102 cm^{-1} for the samples is well known for ether groups in AGE.[41] Also, the peak around ~1093 cm^{-1} may be attributed to the stretching vibration of R–O (alkoxy) in the AGE.[41] Thus, the FTIR has confirmed the presence of hydrophilic GPE components in various samples by indication of the (O–H) stretching vibrations, which seems to increase with increasing the hydrophilic component in the mixtures. The shifts also indicate the possible formation of new bonds within the matrices.

4.3 | Vulcanization properties

The curing parameters: maximum torque (M_H), minimum torque (M_L), change in torque ($\Delta M = M_H – M_L$), onset of cure time (t_{s2}), optimum cure time (t_{90}), and curing rate index (CRI = $100/(t_{90} – t_{s2})$) of the various compounds were extracted from the rheo-curves, analyzed and are presented in Table 2.

Increasing the content of the GECO generally seems to increase the value of viscosity index (M_L), mechanical strength index (M_H), and network density index ($\Delta M = M_H$-M_L) respectively. The formation of tighter structures (–C–S_x–C–) due to the reaction of double bonds (–C=C–) of the allyl glycidyl ether (AGE) and the sulfur curatives is possible. This bond was increased as the GECO content was increased in the presence of the reinforcing particles. For example, SR1 (70 phr of GECO) obtained more than 100, 111, 23, and 72% growth in the M_H value than SR2 (40 phr of GECO), SR3 (40 phr of GECO), SRX (30 phr of GECO), and SRN (40 phr of GECO) respectively. Formation of further tighter structures may be possible by the reaction between the added PEO (PEO-k) and the PEO originally existing within the structure of GECO (PEO-m). Furthermore, the presence of the hydrogen bonds ($–O^{\sigma-}$-----$H^{\sigma+}$–) between the oxygenated backbone of the matrices and the fillers might improve the interactions enough for to increase the torque properties (M_L, M_H, and ΔM) of the composition. The numerous interactions leading to increase in the torque properties is as depicted in the Figure 4.

By comparing, the sulfur-cured compounds (SR1, SRN, and SRX) outperformed those cured with peroxide system (SR2 and SR3) in the measured torque properties due to the strong networks (−C−S_x−C−) from the AGE. With regards to the curing times (t_{s2} and t_{90}), even though some scattering can be seen, it is interesting to observe that increasing the content of the GECO seems to increase the t_{s2} and t_{90} of the WSE composites. The order of decreasing in curing time (t_{s2} and t_{90}) is; SR1 > SR2 > SR3 > SRX > SRN. In particular, SR1 obtained the highest t_{90} value compared to the rest of the compounds. Thus, SR1 was delayed to over 158, 207, 435, and 190% than SR2, SR3, SRX, and SRN respectively. The high oxygenated backbone of GECO in addition to those contributed by PEO and EVA could act as scavengers or cure retarders for the curing of the highly filled GECO compounds. High oxygenated groups were reported to delay the curing time of rubber-graphene oxide-filled composites.[1,42,43] A remarkable observation made was that the CRI of the SRX and SRN was higher or comparable to their counterparts (SR1, SR2, and SR3). This may be due to high filler content (CB and silica) and their modification by silane (TESPT). This increased the tendency for the fillers to disperse well within the matrix and to establish desired filler-polymer interactions, associated with an increase in bound rubber content.[44,45] Similar observation was made with NR-silanized MWCNT by Shanmugharaj et al.[46] EPDM-silanized MWCNT by Khademeh et al.,[47] SSBR-silanized silica by Qu et al[48] and NR-Silanized silica by Hayichelaeh et al.[44] Therefore, curing of the current WSE compositions was greatly dependent on the concentration of the GECO and the filler (silanized CB or silica) present in the matrix.

TABLE 2 Curing properties of the various compositions

Code	M_L (dNm)	M_H (dNm)	$\Delta M = M_H - M_L$ (dNm)	t_{s2} (min)	t_{90} (min)	CRI (min^{-1})
SR1	28.4	56.8	28.4	2.4	20.9	5.4
SR2	10.5	28.3	17.8	0.9	8.1	13.9
SR3	11.4	26.9	15.5	0.9	6.8	16.9
SRX	12.7	45.9	33.2	1.1	3.9	35.7
SRN	13.9	32.9	19.0	1.3	7.2	16.9

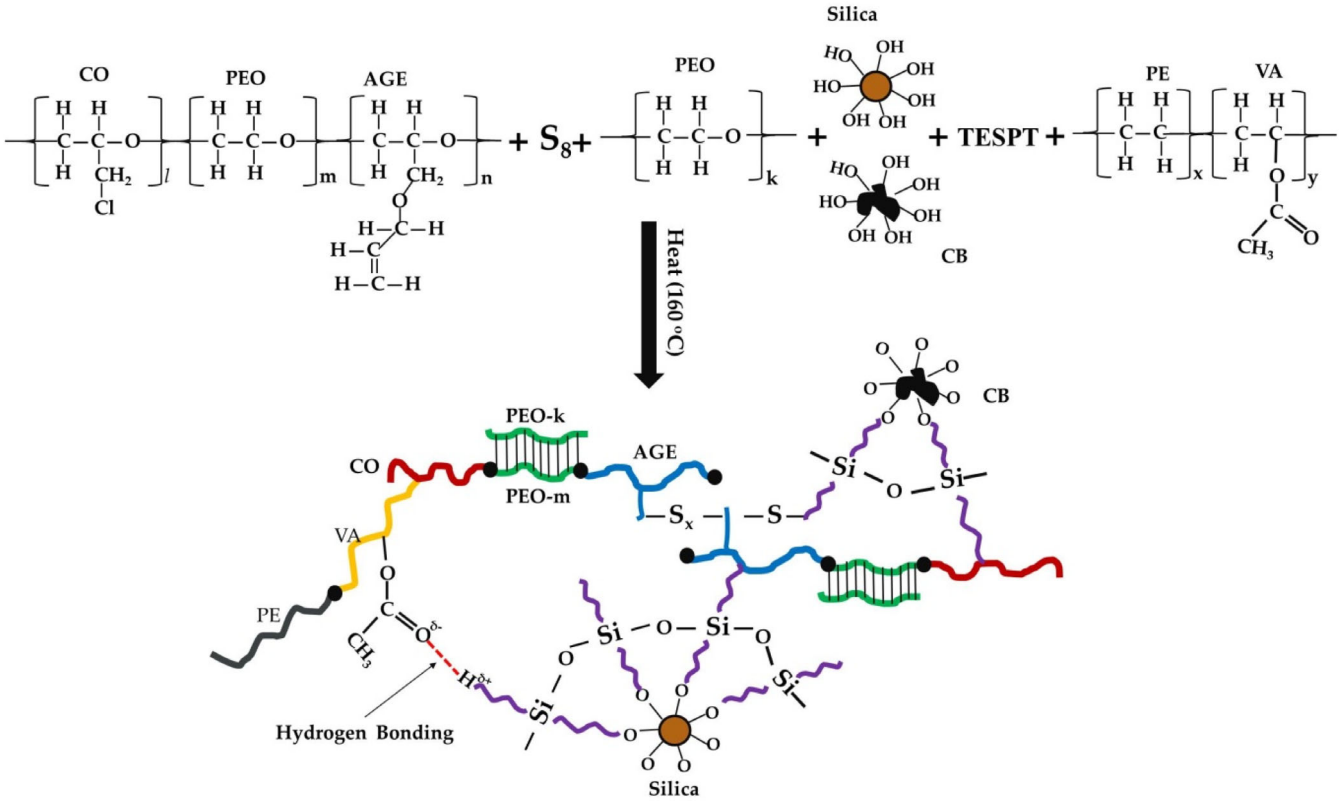

FIGURE 4 Illustration of the vulcanization reaction between GECO, PEO, EVA, and silanized-fillers

4.4 | Crosslinking density analysis

The initial weights (W_i), toluene swelling weights (W_s), swelling ratio (Q_r) [(W_i-W_s)/W_i], and the computed crosslinking density, N(mol cm^{-3}) of the various compounds are presented in Table 3. As seen in Table 3, the strength of the Q_r expressed in percentage in brackets and the reducing order of the N(mol cm^{-3}) values for the compounds which is; SRN > SR1 > SRX > SR3 > SR2, are clearly reported. The order of the N(mol cm^{-3}) shows that there are tighter structures (crosslinks) in SRN than the remaining samples. This may be due to the high content of filler which are coated with the TESPT for effective dispersions and bonding to the matrices.[41,49]

While, increment in N for SRX and SRN may be chiefly due to high filler networks interactions with the matrix, that of SR1 may be greatly due to chemical interactions between double bonds (–C=C–) of the allyl glycidyl ether (AGE) of GECO and the sulfur curatives. Meanwhile, the network structures in SR2 and SR3 seemed to be influenced by high physical networks like hydrogen bonds ($-O^{\sigma-}$-----$H^{\sigma+}$–) between GECO/EVA and the filler particles rather than the chemical networks. Thus, peroxide curatives seem not to favor high chemical networks (N) formation in the presence of GECO/EVA. Therefore, while the water-swelling behavior of the various compounds is expected to follow the order SR2 > SR3 > SRX > SR1 > SRN; an increase in N is expected to improve the physico-mechanical properties of the respective compounds.[1,2,50]

TABLE 3 Crosslinking density properties by equilibrium swelling of the compounds

Code	W_i (g)	W_s (g)	Q_r	N(mol cm^{-3})
SR1	1.461	2.930	1.005476 (100.5%)	7.230×10^{-2}
SR2	1.548	4.215	1.722868 (172.3%)	0.289×10^{-2}
SR3	1.406	3.461	1.461593 (146.2%)	0.523×10^{-2}
SRX	1.802	3.630	1.014428 (101.4%)	5.443×10^{-2}
SRN	1.359	2.720	1.001472 (100.2%)	9.688×10^{-2}

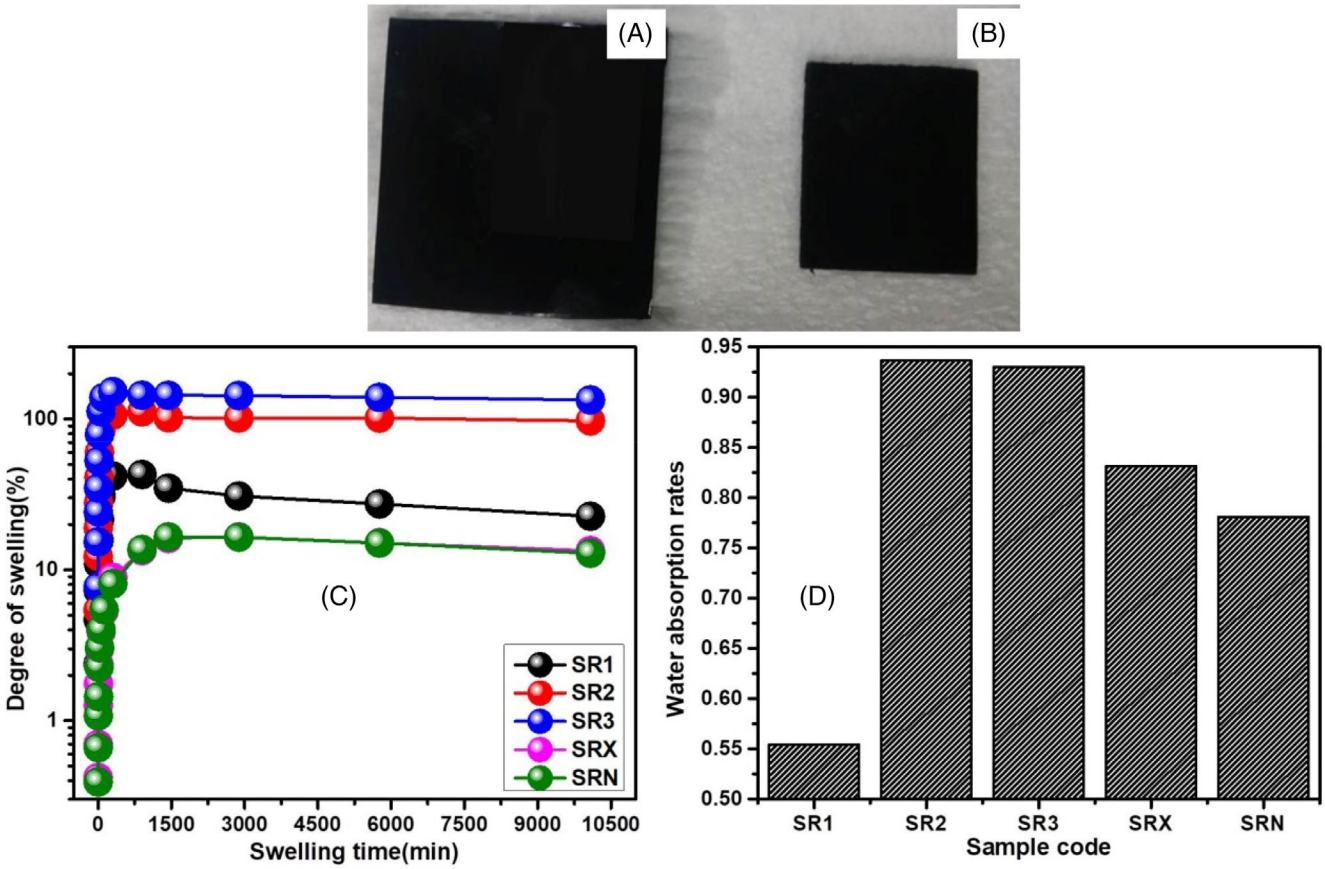

FIGURE 5 A typical image of the type C sample (SR3) in (A) swollen state and (B) non-swollen state. The swelling properties; (C) degree of swelling (%) versus time and (D) absorption rate of samples

4.5 | Water-swelling degree analysis

The typical image of the type C sample (SR3) in swollen state and non-swollen state are as shown in Figure 5A,B respectively while the degree of swelling (%) with respect to time (min) and the rate of water absorption of the derivative compositions prepared from type C (SR1, SR2, SR3, SRX, and SRN) are compared in Figure 5C,D respectively. It was observed from Figure 5C that the swelling degree initially increased to a point and slightly leveled off after prolonged swelling period.

The initial swelling behavior exhibited by the compounds is due to the hydrophilic backbone of GECO, enhanced by the guest polymers (PEO and/or EVA) and fillers, which in all exhibited high affinity or interaction with water molecules via hydrogen-bonding (–$O^{\sigma-}$----$H^{\sigma+}$–) as depicted in Figure 6. The slight drop in the WSE after prolonged swelling may be due to release of the weakly or physically bonded PEO-k (Figure 6.) to the matrix into the water. A sharp drop in water swelling property was observed by Adair et al.[51] for the case of ENR-SAP composite and this were linked to reduction of crosslinking density. However, as clearly seen, the swellability of the current composition was retained at levels which still qualified them as suitable WSE. Comparatively, the effect of PEO in the current composition

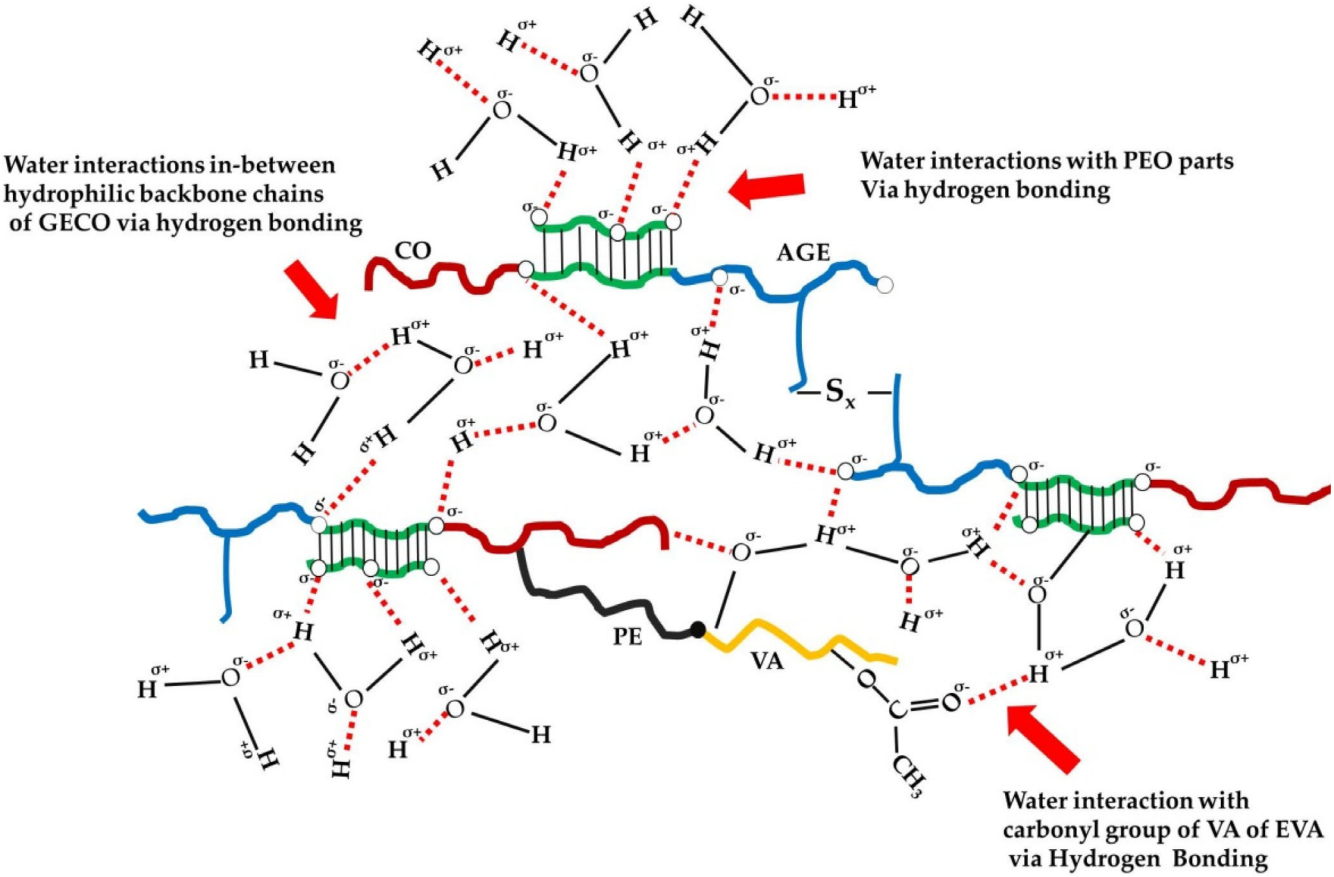

FIGURE 6 Interactions of the hydrophilic backbone of GECO, the guest polymers (PEO and EVA), and fillers in the presence of water via hydrogen bonding

yielded higher water swelling performance than those reported by Adair et al.[51] whose composition (ENR-SAP) swollen in water for 30 days recorded a swelling degree of ~35%.

In addition, the presence of PEO in the samples (SR1–SR3) improved the water swelling behavior compared to those prepared by Yamashita et al.[52] who blended chlorinated polyethylene elastomer with poly (acrylic acid-acrylic amide)[P(AA-M)]. The present work outperformed the swelling properties of ENR-$CaSO_4$ composites which recorded less than 50% water absorption at 20–8°C, reported by Shib et al.[24] In terms of water absorption rates (Figure 5D), the order of decreasing is; SR2 > SR3 > SRX > SRN > SR1. This order corresponds to order of decreasing of equilibrium the swelling degree (Q_r) for SR2 > SR3 but deviates for that of the remaining samples where SR1 > SRX > SRN, as shown in Table 3. It was observed that SR1 containing 70 phr of GECO, 30 phr of PEO, and 0 phr of EVA attained the lowest water absorption rates while SR2 (20phr EVA), SR3 (10 phr EVA), and SRN (5 phr EVA) showed relatively higher absorption rates. Interestingly, SRX which contained 0 phr of EVA still showed better absorption rates compared to SR1 and SRN. This effect may be due to the high content of the carbon black (CB) filler incorporated. Generally, the average filler concentration of the sample was around 15 ~ 25 phr; however, SRX contains 35 phr of filler of which 30 phr is CB. Besides their strong interactions with the polymer chains, it is also possible the high content of filler particles physically opened up the bulk polymer structures with their spherical nature in-between the polymer chains thereby increasing the water absorption rates. Thus, water absorption rates of the compositions were enhanced by high content of EVA or the presence of high filler concentration. Despite the high network densities, the present samples have exhibited higher water absorption rates compared to those earlier reported for chlorinated polyethylene filled with cross-linked poly (sodium acrylate) SAP in the presence of poly(methyl methacrylate-co-Maleic anhydride) compatibilizers[32] and PDMS-based polyuria which uses water for self-healing.[20]

4.6 | Re-usability (second-cycle swelling) study

Re-usability of materials is generally beneficial as it reduces cost and burden of reprocessing of new ones.

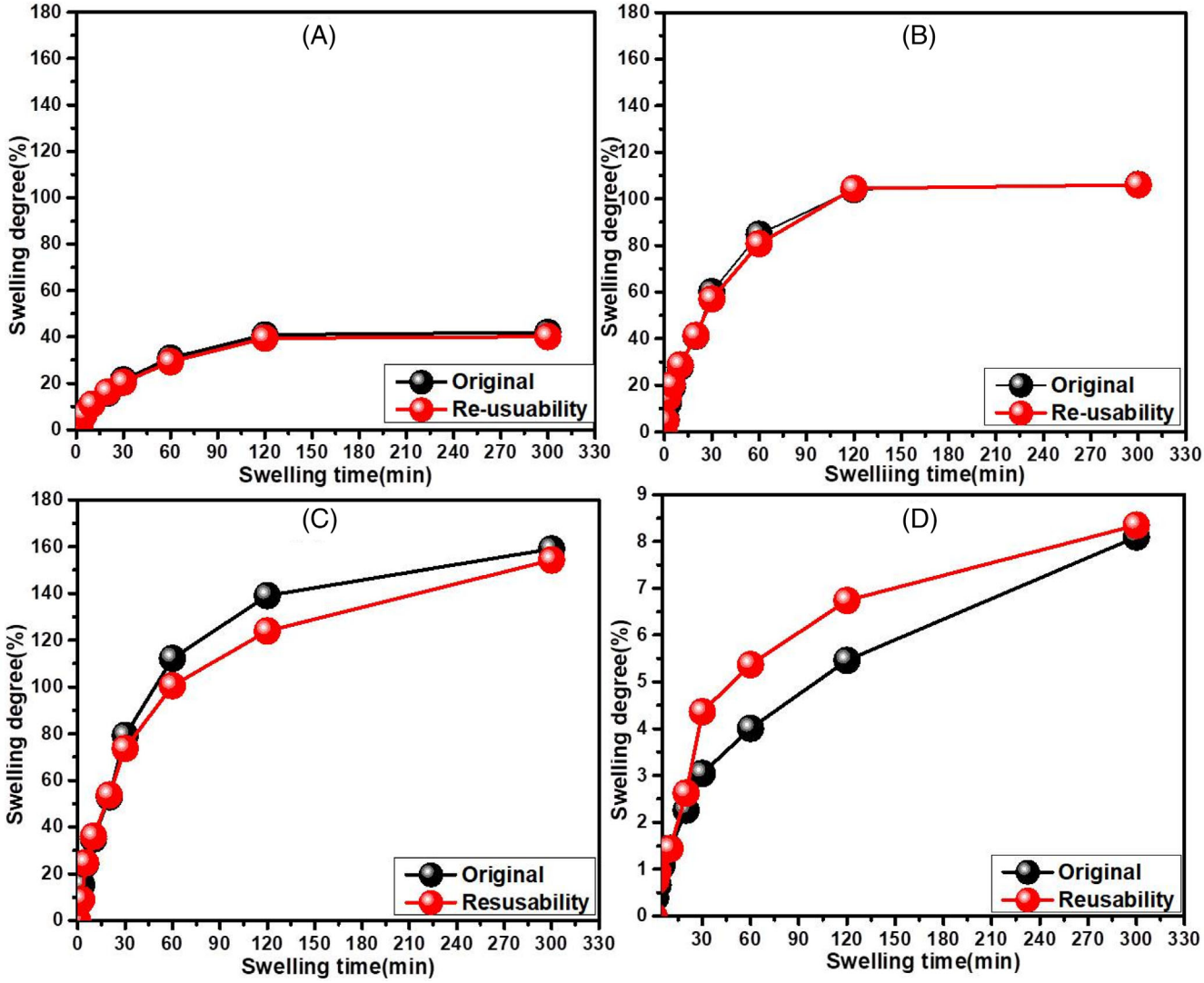

FIGURE 7 Comparing 1st and 2nd cycle of water-swelling behavior of samples; (A) SR1 (B) SR2 and (C) SR3 and (D) SRN

The original swelling ratio and the re-swollen ratio are compared in Figure 7A–D with respect to time (min). As seen in Figure 7A–D, the first and second cycle of swelling generally exhibit a similar correlation.

This may be an indication that only small and morphologically unstable phases of the PEO that were poorly bonded to the main matrix in the presence of the fillers leached out of the matrix during the prolonged water swelling which is an observation common with WSE.[17–19] This slightly reduced the water absorption behavior of the compositions without compromising the overall re-suability performance of the compositions. Hence, the current prepared WSE nanocomposite have shown potentials to be re-used after complete drying by maintaining water-absorption performance and structural integrity.

4.7 | Effect of water swelling on volume expansion

In terms of volume expansion, VE (%), although very small loses can be observed, yet it can be seen in the Figure 8A–D that there exist a strong correlation between the first and second cycle of representative water-swelling samples; SR1, SR2, SR3, and SRN as shown in Figure 8A–D respectively.

These results depicts that, the currently prepared WSE can be re-used to perform the same duty after drying. Accordingly, the samples loaded with a small amount of GPE ratio and with high network density (*N*) experienced the lowest VE (%) due to its tighter network structures. Hence, the currently prepared samples offer many benefits in the future for re-usable water swelling samples for advanced applications.

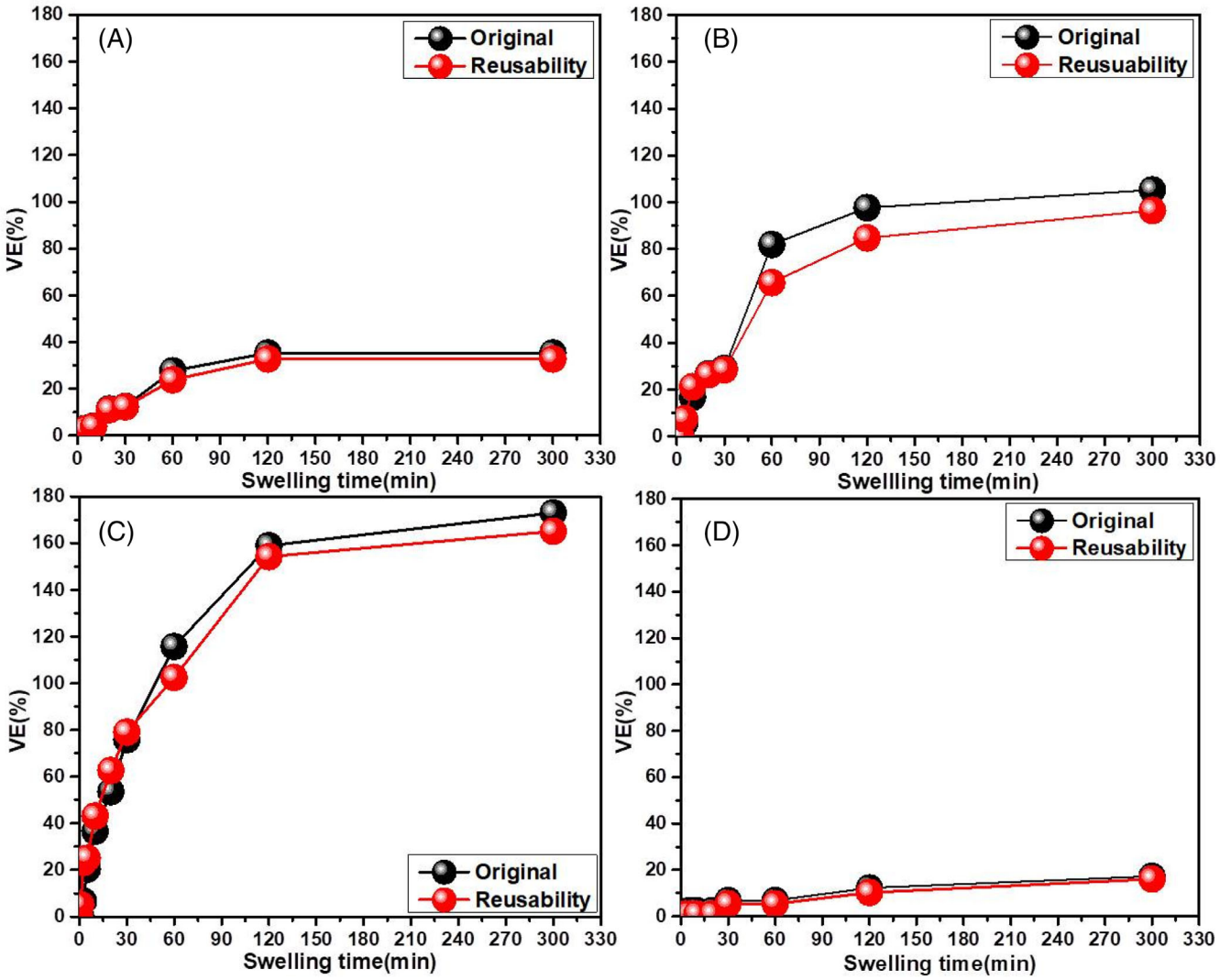

FIGURE 8 Effect of swelling on volume expansion of the samples; (A) SR1 (B) SR2 (C) SR3 and (D) SRN

4.8 | Effect of swelling on physico-mechanical properties

4.8.1 | Tensile strength

The tensile properties of the various WSE samples (SR1-SR3) have been compared in Figure 9A. SR1 leads SR2 and SR3 in tensile strength at values above 55 and 28% respectively before swelling. The tensile strength of the samples drastically dropped as the swelling time increases from 0 to 24 h.

This reducing trend in strength upon swelling may be due to breaking of total network density (both physical and chemical networks) as water leached into bulk matrices, similar to those earlier observed by Adair et al.[51] The order of the effect of water swelling on the decreasing tensile strength of the samples (SR1-SR3) is; SR1 > SR3 > SR2, this followed the decreasing order of network density (*N*); SR1 > SR3 > SR2. With reference to Table 3, SR1 is about 2402 and 1282.4% higher in crosslinking density than SR2 and SR3 respectively, hence SR1 is higher even in extreme swelling state. In Figure 9B SRN outperformed the tensile strength of SRX. Likewise, it is interesting to observe that SRN obtained roughly ~34 and ~80% higher in crosslinking density than SR1 and SRX respectively. Thus, the tensile strength properties of all the samples is directly related to the degree of the crosslinking density, as a result of the nature of the curing agents, filler, and the ratio of the GPE incorporated in the blends. By comparing the samples in Figure 9A,B, it can be seen that prolonged swelling do not seriously decrease the tensile properties of those in Figure 9B, especially for the SRN sample. The reduction of tensile strength of WSE upon prolonged water swelling was also observe by Yamashita et al.[52] In the work of Nakason et al.[53] who prepared water-swellable rubber by blending high-ammonia natural rubber latex with SAPC, PEO, and

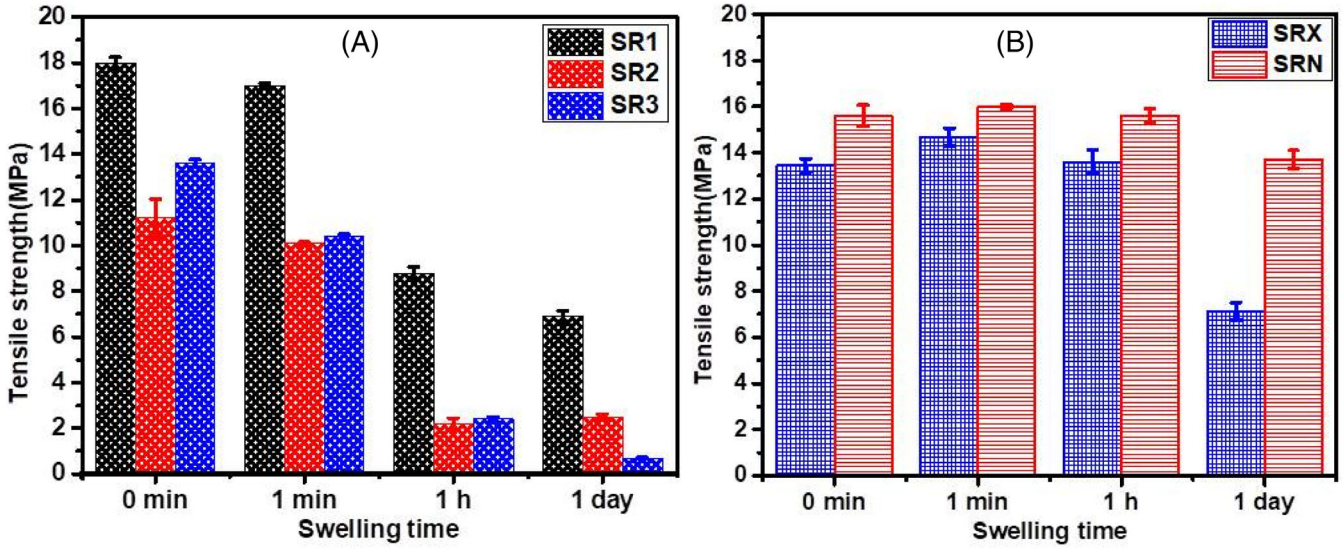

FIGURE 9 Plot of tensile strength (MPa) against swelling time of (A) SR1-SR3 samples and (B) SRX and SRN samples

trimethylolpropane trimethacrylate (TMPTMA). The tensile test results showed that the water swellable rubber containing 10 phr PEO and 2 phr TMPTMA gave a higher mechanical strength of 15.2 MPa which declined upon increasing the PEO loadings (20–40 phr). By comparison, the SR1 (30 phr of PEO) sample obtained a higher mechanical strength of 17.5 MPa in an unswollen state which was maintained around 17 MPa after a min of swelling in water. In addition, Fang et al.[32] reported samples with high water absorption with tensile strength properties converging around below 11 MPa after swelling to equilibrium. This result is lower compared with SRX and SRN of this present work which maintained tensile strength round 14 MPa after 24 h of swelling in water. In general, though, the present compositions (SR1-SR3) have exhibited higher water swelling performance of above 30–140% but with rapid reduction in tensile strength after 24 h of swelling. However, their counterpart SRX and SRN showed moderate water swelling performance above 19% and still maintained tensile strength around ~14 MPa. This result is much better compared to those earlier reported for NR, NBR, SBR, BIIR, and EPDM which recorded tensile strength performance of 1.8–7.0 MPa with equilibrium water swelling values around 6.3–21%[17] and that of hydrophilic PDMS-based polyuria blend which recorded tensile strength lower than 5 MPa.[20]

4.8.2 | Hardness and wear property

Hardness property of the various compositions in their unswollen and swollen state is compared in Figure 10A for SR1–SR3 and Figure 10B for SRX and SRN respectively. By careful examination, it appears the hardness properties of the various samples are greatly influenced by the concentration of filler and that of PEO incorporated. Higher content of filler and PEO seemed to favor high hardness in unswollen state while it dropped upon prolonged swelling in water, especially for compounds with high content of PEO and less filler concentration. Whether swollen or not, the general order of decreasing in hardness for SR1-SR3 samples is; SR1 > SR2 > SR3. In Figure 10B, at the same swelling conditions, SRX (30 phr of CB and 5 phr of silica) shows slightly higher hardness than SRN (25 phr of CB and 3 phr of silica) but the two maintained a steady value around 85 (Shore A) higher than SR1-SR3 samples and those reported earlier for car tread compounds.[37] Thus, the order of increasing in hardness of SR1-SR3 and SRX/SRN generally followed the same order as the chemical crosslinking density (N) from equilibrium swelling and the torque properties; crosslinking density index(ΔM) and the strength index (M_H) obtained from the rheo-curves. Qamar et al.,[54] studied the hardness of the water swelling rubber compounds, a hardness of 73 (Shore A) obtained for the dry sample dropped significantly to hardness of <40 (Shore A), after water swelling. By comparing their results with the current work, it can be seen that SR-SR3 exhibited hardness above 40 (Shore A) while SRX and SRN maintained a steady hardness values around 85 (Shore A) even after 24 h of water swelling.

Therefore, the present compositions have demonstrated relatively better water swelling performance with guaranteed hardness properties. The Figure 10C,D compares the effect of swelling on the wear property of the samples when swollen in water at specific times (0–24 h). It was reported that water-swellable elastomers with high rate of water

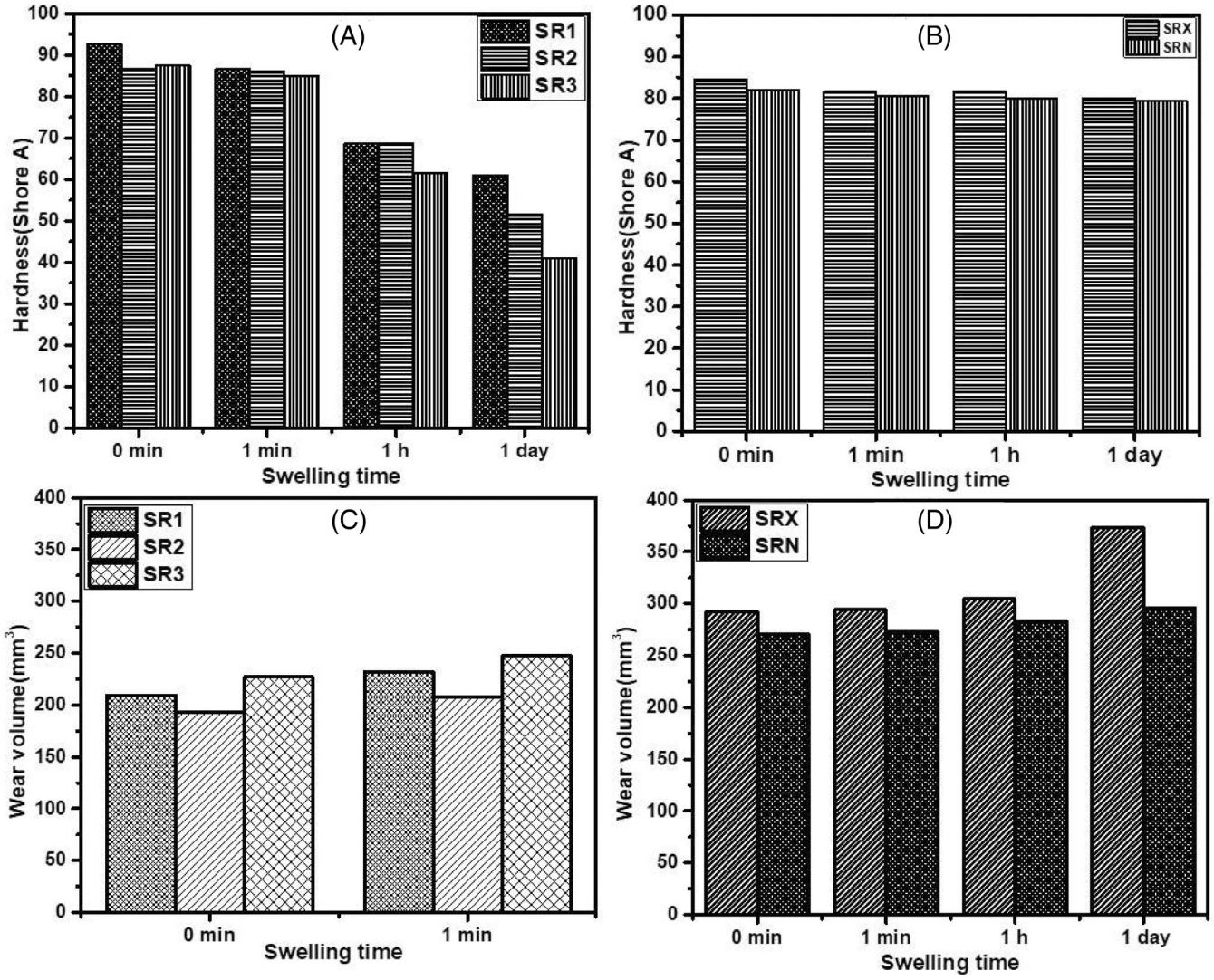

FIGURE 10 A plot of hardness (shore a) versus water swelling time for (A) SR1–SR3 and (B) SRX and SRN samples (C) wear volume versus swelling time for SR1–SR3 and (D) wear volume versus swelling time for SRX and SRN samples

swelling degree experienced rapid increase in volume expansion which could results in wear volume loss.[53,54] Accordingly, in this study, it was observed that as water swelling time increased the wear volume increased. By comparison, SR1-SR3 showed an improvement in wear resistance than their counterparts SRX and SRN, due to desired filler-polymer chain interactions present. The highly filled samples; SRX(30 phr of CB and 5 phr of Silica) and SRN (25 phr of CB and 3 phr of silica) may have high filler-filler interactions with decreased viscoelasticity which in turn increased their wear behaviors.[37]

4.8.3 | Resilience property

The effect of water swelling on the rebound resilience (%) property of the various samples are compared as a function time in Figure 11A,B. Clearly, resilience (%) of the samples generally increased as water-swelling time increased for SR1-SR3 in Figure 11A but remained almost unchanged around ~17% in case of SRX and SRN as shown in Figure 11B. By careful observation, the increment in resilience property of the samples followed the same order as the volume expansion (SR3 > SR2 > SR1) and water swelling degree (SR3 > SR2 > SR1) but showed a reverse behavior as that of the crosslinking density (*N*), hardness and the torque properties (M_H and ΔM). Thus, higher ratio of GPE favored higher water absorption and the increased water absorption resulted in higher volume expansion which in turn increased the ability of the expanded materials to absorbed energy upon striking with the resilience harmer. In particular, sample SR3 recorded over 78% increment in rebound resilience from the unswollen (30%) to 53.5% after

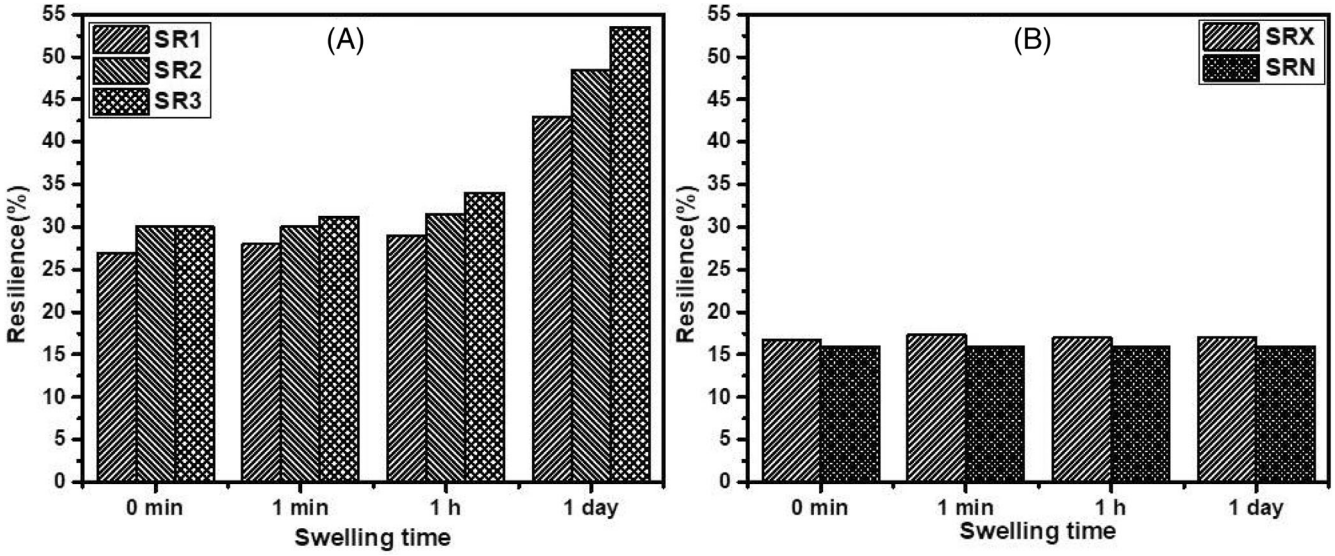

FIGURE 11 Plot of resilience (%) against swelling time of (A) SR1–SR3 samples and (B) SRX and SRN samples

1440 min of swelling in water. Accordingly, samples SRX and SRN (with higher crosslinking density) showed low but stable resilience property compared to sample SR1-SR3. Hence, the present samples have exhibited higher rebound resilience properties compared to those reported earlier by Mensah et al.[37] for compositions consisting of variable blends of ENR/SBR/BR reinforced with mixture of N550/N330 CB, which recorded an average resilience of 27%. Furthermore, the current compositions have shown comparable resilience behavior as the industrial tire tread blends (72 phr NR, 28phr SBR, and 55 phr of N339 CB) which recorded 34.5%[55] and that of the passenger tire tread blend (50 phr of NR, 20 phr SBR, and 20 phr BR with 50phr of N324 CB) which also recorded 20%.[56] Therefore, it can be summarized that the right combination of GPE ratio in a suitable rubber matrix may not only improve water swelling capacity but could also offer benefits in enhancing resilience properties in manufacturing of green tires in the automobile industry.[52,57]

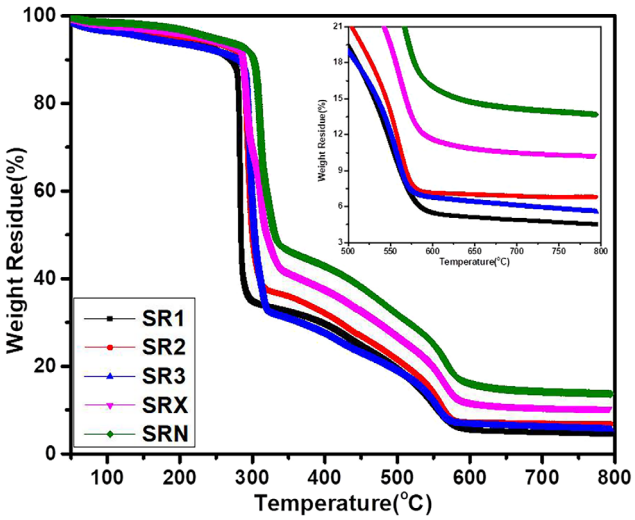

FIGURE 12 Effect of the GPE on the thermal degradation resistance of the water-swellable rubber compounds (SRI, SR2, SR3, SRX, and SRN)

4.9 | Thermal degradation behavior

The weight residue (%) which was used as measure of the thermal resistance of the compositions is plotted as function of temperature in Figure 12 for the various WSE compositions. The decreasing order of thermal decomposition resistance based on the residue (%) is; SRN (13.7%) > SRX (10.3%) > SR2 (6.8%) > SR3 (5.6%) > SR1 (4.5%) as clearly shown as an insert in Figure 12. By comparing the components of the samples; SR1 (70 phr GECO, 30 phr PEO), SR2 (40 phr GECO, 40 phr of PEO, and 20 phr of EVA), and SR3 (40 phr GECO, 50 phr PEO a 10 phr of EVA), it is clear that the thermal resistance of the samples was strongly dependent on the strength of the thermoplastic-toughened rubber matrix phase. The high thermal resistance of SRN than SRX and SR1-SR3 may be ascribed to the combined effect of high crosslinking density and the high content of the thermoplastic-toughened phases present within the structures. Therefore, a high water-swelling performance with high-temperature degradation guarantee will depend on well controlled microstructure of the suitable elastomeric matrix with desired amount of the filler and GPE component, with optimized network density.

5 | CONCLUSION

The preparation of water-swellable rubber nanocomposite material was successfully achieved and carefully investigated. In the end, it was observed that the ratio of (GECO/PEO/EVA) or GPE, the filler content and the nature of curatives are the controlling factors for the differences in curing, swelling, thermal, and other physico-mechanical properties. For instance, high GECO in the composition greatly delayed curing time (t_{s2} and t_{90}) while the desired balance of hydrophilic components GPE increased the torque values (M_H and ΔM), water-swelling, and hardness properties. Meanwhile, the high concentration of reinforcing fillers, especially those coated with the silane (TESPT) might have resulted in effective desired filler-polymer with lower filler-filler networks. The high filler-polymer interaction was confirmed by the increase in the crosslinking density (N) and the tensile properties. For example, SRN obtained about 34 and 80% higher in crosslinking density than SR1 and SRX respectively, while SR1 attained more than 1000% increment in the crosslinking density than the peroxide-cured samples (SR2 and SR3). This result, in combination with the thermoplastic-toughened phases in the matrices determined their respective thermal degradation resistance, of which SRN was the best. It was also observed that the mechanical properties of the water-swellable rubber nanocomposite prepared declined significantly, as the network density decreased during swelling for samples highly filled with GPE in the presence of the reinforcing fillers. Hence, for water swelling performance of elastomers, a suitable balance between GPE and the reinforcing fillers will be necessary for future applications, so as to avoid compromising the physico-mechanical properties. Therefore, the present water-swellable rubber nanocomposites materials with re-usable behavior can find many applications in areas like: wound healing, self-healing pipes, collection of oil spillages in waters, water filtrations, separation of precious metals from liquid substances, and for development of water-based-sensors etc. after careful optimization.

ACKNOWLEDGMENT

Bismark Mensah acknowledges the guidance from the University of Ghana Building a New Generation of Academics in Africa (BANGA-Africa) Project, with funding from the Carnegie Corporation of New York. The assistance offered by Mr Lee of YUTECH Company (South Korea) for granting us access to use their facilities for this work is also acknowledged.

CONFLICT OF INTEREST

The authors declare no competing financial interest. Corresponding author has consent from all co-authors.

DATA AVAILABILITY STATEMENT

The data used to support the findings of this study are available from the corresponding author upon request.

ORCID

Bismark Mensah https://orcid.org/0000-0001-9098-1110

REFERENCES

[1] B. Mensah, K. C. Gupta, H. Kim, W. Wang, K.-U. Jeong, C. Nah, *Polym. Test.* **2018**, *68*, 160.
[2] B. Mensah, H. G. Kim, J.-H. Lee, S. Arepalli, C. Nah, *Int. J. Smart Nano Mater.* **2015**, *6*, 211.
[3] T. P. Selvin, J. Kuruvilla, T. Sabu, *Mater. Lett.* **2004**, *58*, 281.
[4] B. Mensah, S. Kim, S. Arepalli, C. Nah, *J. Appl. Polym. Sci.* **2014**, *131*, 40640.
[5] C. S. Boland, U. Khan, C. Backes, A. O'Neill, J. McCauley, S. Duane, R. Shanker, Y. Liu, I. Jurewicz, A. B. Dalton, J. N. Coleman, *ACS Nano* **2014**, *8*, 8819.
[6] S. Tadakaluru, W. Thongsuwan, P. Singjai, *Sensors* **2014**, *14*, 868.
[7] S. Yang, N. Lu, *Sensors* **2013**, *13*, 8577.
[8] E. Wang, M. S. Desai, S. W. Lee, *Nano Lett.* **2013**, *13*, 2826.
[9] B. Mensah, D. S. Konadu, B. Agyei-Tuffour, *Int. J. Polymer Sci.* **2022**, *2022*, 8038386.
[10] X. Wen, J. Xu, H. Wang, Z. Du, S. Wang, X. Cheng, *Polym. Eng. Sci.* **2022**, *62*, 3132.
[11] S. Araby, Q. Meng, L. Zhang, H. Kang, P. Majewski, Y. Tang, J. Ma, *Polymer* **2014**, *55*, 201.
[12] T. D. Dao, H. I. Lee, H. M. Jeong, *J. Colloid Interface Sci.* **2014**, *416*, 38.
[13] Y. He, Y. Tang, *J. Theor. Comput. Chem.* **2013**, *12*, 1350011.
[14] M. Zanzi, E. Souza, K. Paiva, J. Oliveira, A. Monteiro, G. Barra, G. Dutra, *Polym. Eng. Sci.* **2021**, *61*, 3001.
[15] F. Shahzad, S. Yu, P. Kumar, J.-W. Lee, Y.-H. Kim, S. M. Hong, C. M. Koo, *Compos. Struct.* **2015**, *133*, 1267.
[16] J. J. Edayadiyil, J. Abraham, S. Rajeevan, S. C. George, *J. Polym. Res.* **2021**, *28*, 1.
[17] L. M. Polgar, F. Fallani, J. Cuijpers, P. Raffa, A. A. Broekhuis, M. V. Duin, F. Picchioni, *Rev. Chem. Eng.* **2019**, *35*, 45.
[18] D. Saijun, C. Nakason, A. Kaesaman, P. Klinpituksa, *Songklanakarin J. Sci. Technol.* **2009**, *31*, 561.
[19] N. Dehbari, Y. Tang, *J. Appl. Polym. Sci.* **2015**, *132*, 42786.
[20] P. Zhao, M. Cao, C. Liu, Y. Dai, Y. Tan, S. Ji, H. Xu, *ACS Appl. Mater. Interfaces* **2022**, *14*, 27413.
[21] N. Dehbari, J. Tavakoli, J. Zhao, Y. Tang, *J. Appl. Polym. Sci.* **2017**, *134*, 44548.
[22] N. Dehbari, J. Zhao, R. Peng, Y. Tang, *J. Mater. Sci.* **2015**, *50*, 5157.
[23] S. Moser, Y. Feng, O. Yasa, S. Heyden, M. Kessler, E. Amstad, E. R. Dufresne, R. Katzschmann, R. Style, *Soft Matter* **2022**, *18*, 7229.
[24] S. S. Banerjee, S. Hait, T. S. Natarajan, S. Wießner, K. W. Stöckelhuber, D. Jehnichen, A. Janke, D. Fischer, G. Heinrich, J. J. C. Busfield, A. Das, *J. Phys. Chem. B* **2019**, *123*, 5168.
[25] T. S. Natarajan, S. Okamoto, K. W. Stöckelhuber, S. Wießner, U. Reuter, D. Fischer, A. K. Ghosh, G. Heinrich, A. Das, *ACS Appl. Mater. Interfaces* **2018**, *10*, 16148.
[26] S. S. Banerjee, T. S. Natarajan, B. E. Subramani, S. Wießner, A. Janke, G. Heinrich, A. Das, *J. Appl. Polym. Sci.* **2020**, *137*, 48344.

[27] M. Vaniev, S. Lopatina, N. Sychev, Y. Savchenko, A. Bruk, I. Novakov, *Rubber Chem. Technol.* **2021**, *94*, 591.
[28] G. Wang, M. Li, X. Chen, *J. Appl. Polym. Sci.* **1998**, *68*, 1219.
[29] P. Nuinu, S. Srichan, A. Ngamlerd, C. Wichian, S. Prasertsri, S. Saengsuwan, N. Hinchiranan, C. Vudjung, *Polym. Eng. Sci.* **2022**, *62*, 1833.
[30] J. H. Park, D. Kim, *J. Appl. Polym. Sci.* **2001**, *80*, 115.
[31] C. Liu, J. Ding, L. Zhou, S. Chen, *J. Appl. Polym. Sci.* **2006**, *102*, 1489.
[32] Z. Fang, X. Zhang, M. Xia, W. Luo, H. Hu, Z. Wang, P. He, Y. Zhang, *Adv. Polym. Technol.* **2018**, *37*, 3650.
[33] P. J. Flory, J. Rehner Jr., *J. Chem. Phys.* **1943**, *11*, 512.
[34] G. M. Bristow, W. F. Watson, Cohesive energy densities of polymers. Part 1? Cohesive energy densities of rubbers by swelling measurements, **1958**.
[35] B. Moon, J. Lee, S. Park, C.-S. Seok, *Polymer* **2018**, *10*, 658.
[36] J. Nagode, C. Roland, *Polymer* **1991**, *32*, 505.
[37] B. Mensah, B. Agyei-Tuffour, E. Nyankson, Y. D. Bensah, D. Dodoo-Arhin, J. K. Bediako, B. Onwona-Agyeman, A. Yaya, *Int. J. Polymer Sci.* **2018**, *2018*, 2473286.
[38] T. S. Natarajan, K. W. Stöckelhuber, M. Malanin, K. Eichhorn, P. Formanek, U. Reuter, S. Wießner, G. Heinrich, A. Das, *ACS Omega* **2017**, *2*, 363.
[39] M. Tawfic, A. Hussein, *Kautsch. Gummi. Kunstst.* **2015**, *9*, 30.
[40] I. Pucić, T. Jurkin, *Radiat. Phys. Chem.* **2012**, *81*, 1426.
[41] M. A. López-Manchado, B. Herrero, M. Arroyo, *Polym. Int.* **2004**, *53*, 1766.
[42] B. Mensah, D. Kumar, D. K. Lim, S. Kim, B. H. Jeong, C. Nah, *J. Appl. Polym. Sci.* **2015**, *132*, 42457.
[43] B. Mensah, K. C. Gupta, G. Kang, H. Lee, C. Nah, *Polym. Test.* **2019**, *76*, 127.
[44] C. Hayichelaeh, L. A. E. M. Reuvekamp, W. K. Dierkes, A. Blume, J. W. M. Noordermeer, K. Sahakaro, *Rubber Chem. Technol.* **2017**, *90*, 651.
[45] S. Qian, J. Huang, W. Guo, C. Wu, *J. Macromol. Sci. Part B* **2007**, *46*, 453.
[46] A. Shanmugharaj, J. Bae, K. Lee, W. Noh, S. Lee, S. Ryu, *Compos. Sci. Technol.* **2007**, *67*, 1813.
[47] F. Khademeh Molavi, S. Soltani, G. Naderi, R. Bagheri, *Polyolefins J.* **2016**, *3*, 69.
[48] L. Qu, G. Yu, X. Xie, L. Wang, J. Li, Q. Zhao, *Polym. Compos.* **2013**, *34*, 1575.
[49] J. W. T. Brinke, S. C. Debnath, L. A. E. M. Reuvekamp, J. W. M. Noordermeer, *Compos. Sci. Technol.* **2003**, *63*, 1165.
[50] J. Tu, X. Shi, Y. Jing, H. Zou, J. Kadlcak, Z. Yong, S. Liu, G. Liu, *Polym. Eng. Sci.* **2021**, *61*, 2213.
[51] A. Adair, A. Kaesaman, P. J. P. I. R. Klinpituksa, *Prog. Rubber Plast. Recycl. Technol.* **2020**, *36*, 63.
[52] Y. Zhang, P. He, Q. Zou, B. J. J. O. A. P. S. He, *J. Appl. Polymer Sci.* **2004**, *93*, 1719.
[53] C. Nakason, Y. Nakaramontri, A. Kaesaman, W. Kangwansukpamonkon, S. J. E. P. J. Kiatkamjornwong, *Eur. Polymer J.* **2013**, *49*, 1098.
[54] S. Qamar, T. Pervez, M. Akhtar, M. Al-Kharusi, Material behavior of water-swelling and oil-swelling elastomers, International Conference on Applied Mechanics, Materials and Manufacturing (ICAMMM-2010), **2010**, pp. 13–15.
[55] M. Bijarimi, Z. Hassan, M. Beg, *J. Appl. Sci.* **2010**, *10*, 1345.
[56] H. Atashi, M. Shiva, *Asian J. Chem.* **2010**, *22*, 7519.
[57] P. He, Y. Zhang, R. J. J. O. A. P. S. Hu, *J. Appl. Polymer Sci.* **2007**, *104*, 2637.

How to cite this article: B. Mensah, E. Oduro, *Polym. Eng. Sci.* **2023**, *63*(3), 738. https://doi.org/10.1002/pen.26239